

Screw Geometry Meets Bandits: Incremental Acquisition of Demonstrations to Generate Manipulation Plans

Dibyendu Das¹, Aditya Patankar², Nilanjan Chakraborty², C. R. Ramakrishnan¹, and IV Ramakrishnan¹

Abstract—In this paper, we study the problem of methodically obtaining a sufficient set of kinesthetic demonstrations, one at a time, such that a robot can be confident of its ability to perform a complex manipulation task in a given region of its workspace. Although Learning from Demonstrations has been an active area of research, the problems of checking whether a set of demonstrations is sufficient, and systematically seeking additional demonstrations have remained open. We present a novel approach to address these open problems using (i) a screw geometric representation to generate manipulation plans from demonstrations, which makes the sufficiency of a set of demonstrations *measurable*; (ii) a sampling strategy based on PAC-learning from multi-armed bandit optimization to evaluate the robot’s ability to generate manipulation plans in a subregion of its task space; and (iii) a heuristic to seek additional demonstration from areas of weakness. Thus, we present an approach for the robot to incrementally and actively ask for new demonstration examples until the robot can assess with high confidence that it can perform the task successfully. We present experimental results on two example manipulation tasks, namely, pouring and scooping, to illustrate our approach. A short video on the method: <https://youtu.be/R-qICdEos>

I. INTRODUCTION

The ability to perform manipulation tasks is key to the use of robots in many application areas, including flexible manufacturing, service robotics, and assistive robotics. Complex manipulation tasks, such as opening drawers, pouring, scooping, etc., require the motion of the end effector to be constrained during the execution of the task. It is often hard to manually specify the complete set of constraints for each task. One popular approach is to generate the manipulation plans (a sequence of configurations of the robot’s manipulators such as its arms and grippers) directly based on a set of human-provided *demonstrations*. Such demonstrations can be obtained from video, teleoperation, kinesthetic manipulation of the robot’s end effector, or simulations in virtual or augmented reality, e.g., see [1]–[13]. Despite this rich history, the problem of evaluating the *sufficiency* of a given set of demonstrations and systematically *seeking* additional human-provided demonstrations has remained open.

Our Setting: We focus on manipulation tasks with rigid objects in a tabletop environment where all task-relevant objects are located within a *work area* (see Figure 1).

*This work was partially supported by the US Department of Defense through ALSRP under award No. HT94252410098, SBU OVPR under award no. 93214, and SUNY RF under award no. 95216.

¹Dept. of Computer Science, Stony Brook University, USA. {didas, cram, ram}@cs.stonybrook.edu.

²Dept. of Mech. Engg., Stony Brook University, USA. {aditya.patankar, nilanjan.chakraborty}@stonybrook.edu.

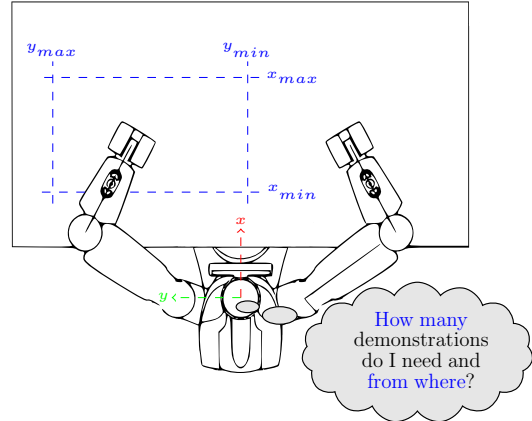


Fig. 1: Schematic sketch of a robot working in a table-top environment. The work area is indicated by the dashed rectangle.

The work area lies entirely within the robot’s reachable workspace. We assume that *positions* and *orientations* (i.e., *poses*) of task-relevant objects are known, possibly informed by vision and other sensor systems.

Demonstrations are provided *kinesthetically*, where a human teacher holds the robot’s arm and the end effector to perform the demonstrated task. Although resource intensive, kinesthetic teaching is generally considered more usable and has a higher task success rate [1], [12]. We restrict our attention to path-based task constraints (e.g. pulling a door by rotating it around its axis, holding a cup upright until it is rotated to pour out its contents into a bowl).

Our Approach: Clearly, without an explicit specification of task constraints, it is impossible to determine whether or not a given manipulation plan satisfies the constraints. This encapsulates the core difficulty in attaching any rigorous measure of *sufficiency* to a set of demonstrations. The key aspect of our approach that helps us circumvent this difficulty is that we generate manipulation plans from a kinesthetic demonstration via screw-linear interpolation, ScLERP [14], [15]. Manipulation plans generated by ScLERP combined with Jacobian-pseudoinverse [16] implicitly preserve the task-related constraints present in the demonstration (see § II). Since the satisfaction of task constraints are assured, a demonstration is sufficient for a given task instance if the plan can be generated while ensuring that the joint limits of the manipulator are also satisfied. This gives us a concrete way to measure the sufficiency of a set of demonstrations.

Let n denote the number of task-relevant objects. The pose of each object is an element of $SE(3)$, the group of rigid body configurations or motions. Let $\mathcal{X} \subseteq SE(3)^n$ be a set of possible poses of the n task-relevant objects. Each element of

\mathcal{X} is a *task instance*. Given \mathcal{X} , and a threshold $\beta \in [0, 1]$, we say that a set of demonstrations is sufficient if the probability that we can generate successful manipulation plans for task instances uniformly drawn from \mathcal{X} exceeds β . (see §III).

Note that such a probability-based measure is, by itself, *coarse*: while a set of demonstrations may be sufficient for \mathcal{X} , there may be regions within \mathcal{X} where we are unable to generate any successful plan! To identify such regions of weakness, we develop a procedure based on PAC (“Probably Approximately Correct”) learning techniques from the “Multi-armed Bandit optimization” literature. We partition \mathcal{X} into a finite set of disjoint regions $\mathcal{X}_j : 1 \leq j \leq K$ for a given natural number K . We draw samples from \mathcal{X}_j to estimate the probability of generating successful manipulation plans for task instances in the j -th region. PAC-learning in this setting lets us determine the maximum number of samples needed in each region to obtain probability estimates with high confidence [17].

An \mathcal{X}_j with a low estimated probability of generating successful manipulation plans is a candidate for the next demonstration. We can now prompt the human teacher *where* to provide the next demonstration. Thus, we can incrementally seek demonstrations until \mathcal{X} is covered: i.e. we can successfully generate manipulation plans with high probability within each subregion \mathcal{X}_j .

Key Contributions:

- 1) We define a concrete measure of *sufficiency* of a set of demonstrations from which we can generate manipulation plans for a given set of task instances (§IV).
- 2) We provide a sampling procedure to estimate the sufficiency measure for subregions of the given set of task instances (§V). This provides a basis for seeking additional demonstrations from the human teacher.
- 3) We present experimental results on two complex manipulation tasks: **scooping** and **pouring**, to show that only a few examples (less than 8) are sufficient to generate successful plans over a specified work area (§VI).

We begin the technical development in this article with a more detailed description of the closely related work.

II. RELATED WORK

Manipulation tasks, such as pouring from a container or opening a hinged door, involve constraints on motion. Such constraints are hard and often impossible to specify generically with soundness or completeness guarantees. Learning from Demonstrations (LfD) [2], [3], [18] avoids this problem by using a set of demonstrations provided *a priori* to generate a constrained motion. This naturally raises two questions: 1) whether plans for motion plans generated from demonstrations indeed satisfy the implicit constraints of the given task, and 2) whether a set of demonstrations are sufficient to generate robust motion plans for tasks in a specified work area.

A. Motion planning from demonstrations

There are a wide variety of techniques for generating motion plans from demonstrations, including probabilistic

models based on hidden Markov models (HMM) [19], Gaussian mixture models (GMM) [20], and bio-inspired techniques based on dynamical systems such as dynamical movement primitives (DMP) [21]–[24]. However, these works attempt to mimic the demonstrations regardless of aspects that are crucial and meaningful to the implicit task constraints. Hence, there is no formal way to establish that a generated plan is correct for the given task.

An important class of task constraints are restrictions on the path of the end effector or manipulated object. Holding an open container upright when moving it, pulling a door in a circle around its hinge, etc., are examples of path-based task constraints. Our earlier work has developed methods based on screw linear interpolation, ScLERP [14], [15] to generate motion plans in a subspace of the task space that preserves path-based task constraints implicit in the demonstrations. By focusing on the parts of the trajectory close to the objects of interest, these works pay particular attention to the constraints most relevant to the task. Two additional points on ScLERP-based motion plan generation are noteworthy. First, planning in the task space implies that the same demonstrations can be used to generate plans for various robot configurations (varied degrees of freedom, joint lengths, etc.). Second, planning is done online, ensuring that the generated plan is executable by a given robot arm (i.e. satisfies joint limits and constraints).

B. Demonstration sufficiency using self-evaluation

The high-level objective of our work is to develop a framework in which the robot can *self-evaluate* its ability to generate low-level motion plans using a few demonstrations for complex manipulation tasks such as pouring, scooping, etc. This enables the robot to methodically seek additional demonstrations at targeted locations until it achieves a threshold of confidence in plan generation.

Previous works on self-evaluation of the satisfiability of task-related constraints [25], [26], have focused mainly on sensor information available from a perception system [27], [28] or high-level task specification [29]. However, none of the existing work on self-evaluation can be used to evaluate the robot’s confidence in manipulation plan generation using kinesthetic demonstrations.

A recent work [30] in the context of navigation tasks looks at the problem of *demonstration sufficiency* by doing *autonomous assessment*. However, in that work, a demonstration is phrased as expert-provided directions required to successfully navigate a 2D grid environment, which does not apply in the setting of manipulation problems because in manipulation, task constraints are embedded in the entire trajectory of the demonstration.

III. SCREW-GEOMETRY BASED MOTION PLANNING

We first describe the pertinent mathematical background along with motion planning based on screw geometry from demonstrations, which will allow us to formally define our problem in §IV.

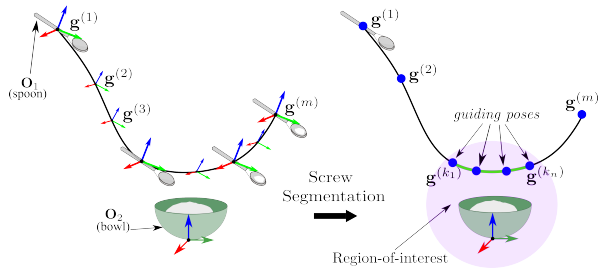


Fig. 2: Overview of the motion segmentation algorithm [15] for scooping the contents from a bowl using a spoon. **Left:** The human-provided demonstration is shown as a sequence of poses (of the spoon) in $SE(3)$, along with the pose of the bowl. **Right:** Segmenting the sequence of poses in $SE(3)$ into a sequence of guiding poses. Each pair of consecutive guiding poses forms a constant screw segment. The task-relevant constraints are the sequence of constant screw segments in a region of interest surrounding the task-related object, bowl.

A. Task Instance

The reference frame fixed to the link of the robot arm beyond the last joint or on any object that is rigidly held by the robot is called the *end effector frame*. The *pose of the end effector* refers to the position and orientation of the end effector frame. We consider manipulation planning tasks where the task specification includes the initial pose of the end effector and the poses of other task-relevant objects that determine the end effector’s goal pose. Let $\mathcal{X} \subset SE(3)^n$ be a compact set, where n is a positive integer representing the total number of task-relevant objects, including the object held by the robot. For a given manipulation task, an *instance of the task* is defined by $\mathbf{x} \in \mathcal{X}$. Thus, the set \mathcal{X} defines the set of all task instances for a given task. We assume that all task-relevant objects are within the set of all reachable poses of the robot’s end effector.

B. Kinesthetic Demonstration and its Representation

For any manipulation task, there may be constraints on the end-effector’s path that characterize the essential characteristics of the manipulation task. A kinesthetic demonstration of a task, given by holding the hand of the robot in a zero-gravity mode, traces an end-effector path that satisfies the task constraints. Let $\mathcal{J} \subset \mathbb{R}^d$ be the *joint space*, i.e., the set of all possible joint configurations of the robot, where d is the number of joints of the robot’s manipulator arm. For a manipulation task instance, $\mathbf{y} \in \mathcal{X}$, a kinesthetic demonstration, Θ , is recorded as a *discrete sequence of points from a joint space path*, i.e., a sequence of joint angle configurations $\Theta = \langle \theta^{(1)}, \dots, \theta^{(m)} \rangle$, where $\theta^{(j)} \in \mathcal{J}$, $j = 1, 2, \dots, m$, is a vector of dimension d , whose i -th component, $\theta_i^{(j)}$, represents the i -th joint angle of the robot arm. Every demonstration instance, Θ , is associated with a task instance \mathbf{y} . We keep this association implicit to avoid notational clutter.

Using a single demonstration to represent the task space motion constraints in the joint space is statistically ill-posed since the (position inverse kinematics) mapping from the task space to the joint space is multi-valued (especially for redundant manipulators). Typically, any joint space-based technique uses multiple demonstrations, and it is usually

difficult to *a priori* specify the number of demonstrations required to learn the task space constraints. Therefore, we use a task space representation of the demonstration, which allows us to extract the motion constraints in the task space from a single demonstration by exploiting the screw-geometric structure of motion [15].

More specifically, following [15], each joint configuration, $\theta^{(j)}$, is mapped to a pose of the robot’s end effector frame, $\mathbf{g}^{(j)} \in SE(3)$, using position forward kinematics. Thus, the demonstration is a path, i.e., a sequence of poses in $SE(3)$, given by $\mathcal{G} = \langle \mathbf{g}^{(1)}, \dots, \mathbf{g}^{(m)} \rangle$. By decomposing the path \mathcal{G} into a sequence of constant screw segments, we obtain the representation of the demonstration as a sequence of guiding poses $\Gamma = \langle \mathbf{g}^{(1)}, \dots, \mathbf{g}^{(k_1)}, \mathbf{g}^{(k_2)}, \dots, \mathbf{g}^{(m)} \rangle$. Figure 2 shows a schematic sketch of this process, and the details are presented in [15]. Note that Γ is a subsequence of \mathcal{G} and two consecutive poses in Γ represent a constant screw motion or a one-parameter subgroup of $SE(3)$.

The screw-geometric representation exploits the physical structure of motion implied by Chasles’ theorem that *any path in $SE(3)$ can be arbitrarily closely approximated by a sequence of constant screw segments or one-parameter subgroups of $SE(3)$* . Thus, even one example is sufficient to extract the constant screw segments.

C. Motion Planning from a Single Demonstration and Evaluation of Motion Plan

We will use the two-step motion planner discussed in [15] to generate motion plans for new task instances that differ from the demonstration instance. In particular, we will denote such a motion plan generator by `hasMotionPlan`(\mathbf{x}, Γ) which takes as input any task instance \mathbf{x} , a demonstration Γ and decides whether or not a motion plan can be generated for \mathbf{x} using Γ . The process of plan generation involves (a) transferring the guiding poses, Γ , to a new set of guiding poses, Γ' , to account for the new poses of the task-relevant objects and (b) using screw linear interpolation (ScLERP) to generate the path between two consecutive guiding poses. As proven in [16], ScLERP ensures that the constant screw constraint encoded by two consecutive guiding poses is always satisfied without explicitly enforcing it. Therefore, the planner used in this paper to generate a manipulation plan always ensures that the manipulation constraints are satisfied. However, the motion planner may fail to generate a plan for a given task instance, e.g. due to violation of joint limits.

Thus, we assume that given a demonstration Γ we have a mapping $f_\Gamma : \mathcal{X} \rightarrow \{0, 1\}$, such that, for any new task instance $\mathbf{x} \in \mathcal{X}$, $f_\Gamma(\mathbf{x}) = 1$, if and only if the robot can successfully generate a manipulation plan for the task instance \mathbf{x} using the demonstration Γ . If we consider a set of demonstrations $\mathcal{D} \equiv \{\Gamma_i\}_{i=1}^n$ such that for any $\mathbf{x} \in \mathcal{X}$, $\max_{\Gamma_i} f_{\Gamma_i}(\mathbf{x}) = 1$, then we have a set of demonstration examples such that the robot is guaranteed to generate a manipulation plan for any task instance of a given task.

IV. SELF-EVALUATION

In this section, we formally characterize the sufficiency of a set of demonstrations \mathcal{D} to cover a given set of task instances \mathcal{X} . If \mathcal{D} is considered insufficient by this metric, we describe an approach to identify a region (subset) of \mathcal{X} that contains a good candidate for a new demonstration. This forms the basis for incremental acquisition of demonstrations further developed in §V.

A. Sufficiency of Demonstrations

For a demonstration, Γ_i , let $\mathcal{B}(\Gamma_i, \mathcal{X}) \subseteq \mathcal{X}$, be the set of task instances where Γ_i can be used to generate manipulation plans successfully. Thus,

$$\mathcal{B}(\Gamma_i, \mathcal{X}) = \{\mathbf{x} \in \mathcal{X} \mid f_{\Gamma_i}(\mathbf{x}) = 1\} \quad (1)$$

Let $\text{Vol}(A)$, with $A \subseteq \mathcal{X}$ be a volume measure [31] defined on \mathcal{X} .

Definition 1 (Coverage): The *coverage* of a demonstration Γ_i with respect to a set of task instances \mathcal{X} , denoted by $\mathbb{P}_{\mathcal{X}}(\Gamma_i)$, is defined as:

$$\mathbb{P}_{\mathcal{X}}(\Gamma_i) = \frac{\text{Vol}(\mathcal{B}(\Gamma_i, \mathcal{X}))}{\text{Vol}(\mathcal{X})}$$

Let $\mathcal{D} \equiv \{\Gamma_i\}_{i=1}^n$ be a set of demonstrations. We can lift \mathcal{B} from individual demonstrations to sets of demonstrations. Let $\mathcal{B}(\mathcal{D}, \mathcal{X}) = \bigcup_{i=1}^n \mathcal{B}(\Gamma_i, \mathcal{X})$. Then,

$$\mathcal{B}(\mathcal{D}, \mathcal{X}) = \left\{ \mathbf{x} \in \mathcal{X} \mid \max_{\Gamma_i \in \mathcal{D}} f_{\Gamma_i}(\mathbf{x}) = 1 \right\} \quad (2)$$

Thus, $\mathcal{B}(\mathcal{D}, \mathcal{X})$ is the set of all task instances in \mathcal{X} such that there is at least one demonstration \mathcal{D} that can be used to generate a successful manipulation plan.

Analogously, we can lift the notion of *coverage* to sets of demonstrations:

$$\mathbb{P}_{\mathcal{X}}(\mathcal{D}) = \frac{\text{Vol}(\mathcal{B}(\mathcal{D}, \mathcal{X}))}{\text{Vol}(\mathcal{X})} \quad (3)$$

Definition 2 (Sufficiency): Given a probability threshold $0 \leq \beta \leq 1$, a set of demonstrations \mathcal{D} is said to be *sufficient* for a set of task instances \mathcal{X} with respect to β if

$$\mathbb{P}_{\mathcal{X}}(\mathcal{D}) \geq \beta$$

B. Identification of New Demonstration Candidates

If a set of demonstrations \mathcal{D}_0 is insufficient for task instances \mathcal{X} , we would like to incrementally seek additional demonstrations, one at a time, thereby constructing a sequence of demonstration sets $\mathcal{D}_0, \mathcal{D}_1, \dots$ such that some element of this sequence, say \mathcal{D}_n is sufficient for \mathcal{X} .

We identify a small subset of task instances to seek the next demonstration by partitioning \mathcal{X} into K disjoint compact sets $\mathcal{X}_j : 1 \leq j \leq K$. Note that

$$\mathbb{P}_{\mathcal{X}}(\mathcal{D}, \mathcal{X}) = \frac{\text{Vol}(\mathcal{B}(\mathcal{D}, \mathcal{X}))}{\text{Vol}(\mathcal{X})} = \frac{\sum_j \text{Vol}(\mathcal{B}(\mathcal{D}, \mathcal{X}_j))}{\sum_j \text{Vol}(\mathcal{X}_j)}$$

Then, if $\mathbb{P}_{\mathcal{X}}(\mathcal{D}_i) < \beta$, then there is a partition \mathcal{X}_j such that $\mathbb{P}_{\mathcal{X}_j}(\mathcal{D}_i) < \beta$, that is, \mathcal{D}_i is not sufficient for \mathcal{X}_j . Such a subset \mathcal{X}_j contains candidate task instances for the next demonstration.

C. Formulation as Multi-Arm Bandit Optimization

We pose the problem of identifying the partition \mathcal{X}_j that has the *least coverage*, $\mathbb{P}_{\mathcal{X}_j}(\mathcal{D}_i)$, in terms of the K -arm bandit optimization problem [32]. In the special case of Bernoulli K -arm bandit, each pull of the j -th arm yields

Algorithm 1 Obtaining a Sufficient Set of Demonstrations using Self Evaluation

Input: $K, \mathcal{X}_{1..K}, \beta, \epsilon, \delta, \mathcal{D}_0$ $\triangleright |\mathcal{D}_0| \geq 1$
Output: \mathcal{D}

- 1: $\mathcal{D} \leftarrow \mathcal{D}_0$
- 2: **while** true **do**
- 3: $j^*, \hat{\mu}_{j^*}, \mathcal{T}_{j^*} \leftarrow \text{getBestArm}(K, \epsilon, \delta, \mathcal{X}_{1..K}, \mathcal{D})$
- 4: **if** $\hat{\mu}_{j^*} \leq 1 - \epsilon - \beta$ **then** \triangleright see §V-D
- 5: **break** \triangleright End demonstration acquisition
- 6: $\mathbf{y}^* \leftarrow \text{selectFailedTaskIn}(\mathcal{T}_{j^*})$ \triangleright see §V-B
- 7: $\Gamma \leftarrow \text{getNewDemonstrationAt}(\mathbf{y}^*)$ \triangleright see §V-C
- 8: $\mathcal{D} \leftarrow \mathcal{D} \cup \{\Gamma\}$

a reward of 1 with an (unknown) probability p_j and 0 with probability $(1 - p_j)$. The optimization problem is to find the *best arm*, i.e., the one with the highest expected reward. Algorithms for solving this problem are compared based on the expected number of pulls (samples) needed to determine the best arm. For our problem, we create a K -arm bandit with partitions \mathcal{X}_j comprising the K arms. Pulling the j -th arm corresponds to sampling a task instance \mathbf{x} from \mathcal{X}_j . The reward 1 if $\mathbf{x} \notin \mathcal{B}(\mathcal{D}_i, \mathcal{X}_j)$, i.e. if the current set of demonstrations cannot generate a successful manipulation plan for \mathbf{x} ; and 0 otherwise.

Note that in this formulation, the “best arm” corresponds to the partition that is least covered by \mathcal{D}_i . In other words, the best arm points to the partition where the robot has the least ability and hence should ask for the next demonstration. Once a new demonstration is obtained, the same process is repeated with the updated set of demonstrations \mathcal{D}_{i+1} . We stop when the current set of demonstrations is sufficient for all partitions.

V. INCREMENTAL DEMONSTRATION ACQUISITION USING SELF-EVALUATION

Algorithm 1 codifies our approach to acquire demonstrations one at a time such that the set is sufficient for a given set of task instances \mathcal{X} . The algorithm takes the K partitions of task instances, $\mathcal{X}_{1..K}$, the threshold β to determine sufficiency, and two parameters ϵ and δ , both $\in (0, 1)$, and a non-empty set of initial demonstrations, \mathcal{D}_0 . Each element of the set \mathcal{D}_0 is a sequence of guiding poses, where two consecutive guiding poses constitute a constant screw motion. The algorithm proceeds by adding

Algorithm 2 getBestArm

Input: $K, \epsilon, \delta, \mathcal{X}_{1..K}, \mathcal{D}$
Output: $j^*, \hat{\mu}_{j^*}, \mathcal{T}_{j^*}^1$

- 1: $N \leftarrow \frac{2}{\epsilon^2} \ln \left(\frac{2K}{\delta} \right)$ \triangleright see § V-A
- 2: **for** $j \in \{1, \dots, K\}$ **do**
- 3: $\mathcal{T}_j \leftarrow \{\mathbf{x} \sim \mathcal{U}(\mathcal{X}_j)\}$ s.t. $|\mathcal{T}_j| = N$
- 4: $\mathcal{T}_j^1 \leftarrow \{\mathbf{x} \in \mathcal{T}_j \mid \forall \Gamma \in \mathcal{D}. \neg \text{hasMotionPlan}(\mathbf{x}, \Gamma)\}$
- 5: $\hat{\mu}_j \leftarrow \frac{|\mathcal{T}_j^1|}{|\mathcal{T}_j|}$ \triangleright Estimated expected reward
- 6: $j^* \leftarrow \arg \max_j \{\hat{\mu}_j\}$

new demonstrations, initialized as \mathcal{D}_0 . In each iteration,

- (a) The algorithm first determines the partition j^* that is least covered by the current set of demonstrations (line 3) using bandit optimization as a subroutine (see §V-A). Along with j^* , we also obtain $\hat{\mu}_{j^*}$, the empirical estimate of $1 - \mathbb{P}_{\mathcal{X}_{j^*}}$ for the current set of demonstrations.
- (b) These sample task instances are used to select a suggested task instance \mathbf{y}^* for the next demonstration (line 4); see §V-B for details.
- (c) Based on the suggested instance \mathbf{y}^* , we then obtain a new demonstration from the human teacher (line 5); see §V-C for details.
- (d) The new demonstration is added to the set of current demonstrations (line 6).

The collection of new demonstrations ends when we determine, with high confidence, that the current set of demonstrations is sufficient for every partition (see §V-D).

A. Finding an ϵ -Optimal Arm

Algorithm 2 uses a naïve (ϵ, δ) -PAC learning algorithm to identify an ϵ -optimal arm of our bandit formulation. In this algorithm, \mathcal{T}_j^1 (line 4) is the set of all task instances for which we cannot find a motion plan and hence have reward 1. This algorithm ensures with confidence $1 - \delta$ that the empirical estimate of the expected reward for each arm, $\hat{\mu}_j$, is ϵ -close to the true expected reward μ_j . That is, $\mathbb{P}\left(\max_j \{|\mu_j - \hat{\mu}_j|\} \leq \epsilon\right) \geq 1 - \delta$.

The samples for each arm are drawn from uniformly distributed random task instances in each partition. Since each partition is a subset of $SE(3)$, we can use the techniques described in [33] used for sampling from $SE(3)$. The reward for each sample \mathbf{x} is determined by checking if an executable motion plan can be derived for \mathbf{x} based on the currently available set of demonstrations. We use the ScLERP based motion planner [15] to generate plans for each sample task instance. The ScLERP motion planner generates a set of guiding poses for each given task instance, but may fail to produce a sequence of feasible joint configurations needed to execute the plan even when such feasible configurations exist. This is a fundamental problem due to the inherent difficulty in always finding feasible paths in the joint space via inverse kinematics. Hence, determining rewards via ScLERP motion planner gives us an upper bound of rewards. Nevertheless, this only means that the set of demonstrations we find will be *conservative* — sufficient to cover the task instances — but may not be minimal. The number of samples drawn from each arm, N , needed to ensure the confidence bound, is $\frac{2}{\epsilon^2} \ln\left(\frac{2K}{\delta}\right)$, as shown by a short proof based on the Hoeffding-Chernoff inequality given in the appendix A.

Note that we do not need to estimate each μ_j accurately to identify j^* ; only the expected rewards of arms that are close to optimal need to be evaluated accurately. Several PAC-learning algorithms reduce the number of samples needed to identify an arm that is ϵ -close to optimal with confidence $(1 - \delta)$ [34]. Other techniques such as UCB [35] may also be used to identify j^* . We are currently evaluating the

suitability of such techniques and their effect on incremental demonstration acquisition.

B. Suggestion for the Next Demonstration

Having determined the partition with least coverage, we seek the next demonstration using the following heuristic. Since we use ScLERP-based motion planner to check for feasible motion plans, we know that for each failed task instance (i.e. those in \mathcal{T}_{j^*} with reward 1), there will be a screw segment $(\mathbf{g}^{(i)}, \mathbf{g}^{(i+1)}) \in \mathcal{G}$ such that $\mathbf{g}^{(i)}, \mathbf{g}^{(i+1)} \in \mathcal{G}$ for which we could not find a feasible joint-space path (due to joint limit violations). We choose the failed task instance \mathbf{y}^* for which the joint-limit violation occurred in the earliest screw segment. Intuitively, a task failing early may have fewer viable alternative executions.

C. Obtaining a New Demonstration

A kinesthetic demonstration is collected, as described in § III-B, by recording a discrete sequence of joint angles Θ and extracting from them a sequence of guiding poses Γ . Note that even though we were seeking a demonstration for task instance \mathbf{y}^* , the task instance for the provided demonstration may be different — object poses may differ due to errors in manual placement.

D. Stopping Condition

This incremental process continues until the robot is confident enough that the overall success probability in the entire work area meets or exceeds a chosen threshold β i.e., $\mathbb{P}_{\mathcal{X}}(\mathcal{D}) \geq \beta$. In our setup μ_{j^*} is the (true) probability of failure to generate a successful motion plan in the region \mathcal{X}_{j^*} corresponding to the optimal bandit arm j^* . When $\mu_{j^*} \leq 1 - \beta$, we can then claim with confidence $1 - \delta$ that for each partition \mathcal{X}_j , $\mathbb{P}_{\mathcal{X}_j}(\mathcal{D}_i) \geq \beta$. Note that we only know the empirical estimate $\hat{\mu}_j$ with the constraint $|\mu_j - \hat{\mu}_j| \leq \epsilon$. The *testable* condition used as the stopping condition (line 4 of Alg. 1) is $\hat{\mu}_{j^*} \leq 1 - \epsilon - \beta$ since it implies $\mu_{j^*} \leq 1 - \beta$. When this condition is satisfied, we can claim with confidence $(1 - \delta)$ that the current set of demonstrations \mathcal{D} is sufficient for all task instances in \mathcal{X} .

Note that although μ_{j^*} is monotonically non-increasing, we cannot bound the number of demonstrations needed to satisfy the stopping condition *a priori*. Alternatively, if we use a budget of a maximum number of demonstrations as our stopping criterion or stop early, we can compute the probability $\beta' = 1 - \epsilon - \hat{\mu}_{j^*}$ such that for each partition the robot believes it will be successful with probability β' . Here, $\hat{\mu}_{j^*}$ is the largest empirically estimated failure probability among all the regions in the last iteration.

VI. EXPERIMENTAL RESULTS

We present experimental results for two example manipulation tasks, namely **pouring** and **scooping**. Both tasks are characterized by end-effector motion constraints that must be satisfied for successful manipulation. Fig. 3 shows screenshots of the example demonstrations.

We present three types of experimental results.

First, we illustrate the process of self-evaluation and interactive demonstration acquisition for both pouring and

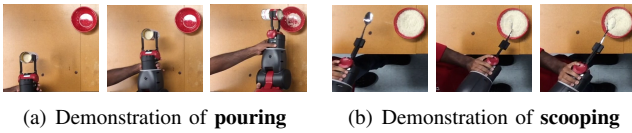


Fig. 3: Snapshots of kinesthetic demonstrations of **pouring** (Fig: 3(a)) and **scooping** (Fig: 3(b)) tasks. In each demonstration, the left frame is the initial pose and the right one is the final pose. We observe that the number of demonstrations required is small, 2 for pouring and 4 for scooping.

Second, to gather further empirical evidence on the number of demonstrations required to perform manipulation tasks with high confidence, we present extensive experimental studies to understand the distribution of the number of demonstrations required and its sensitivity to the choice of K , the number of sub-regions used for sampling in Alg. 1. We find that only a handful of examples, at most 7, are always sufficient.

In the third set of experiments, we use the sufficient set of demonstrations obtained using Alg. 1 to generate plans and execute experimental trials for 64 task instances. We observe that although the demonstrations were obtained based on plans generated in simulations, all of the executed plans satisfied the joint limit constraints.

Experimental Setup: The experiments were performed in a tabletop environment using a Baxter robot from ReThink Robotics. Scooping and pouring are done using a symmetric bowl placed in a rectangular region on the table (Fig. 1). The work area is $0.37m \times 1.02m$ with $x_{\min} = 0.71m$, $x_{\max} = 1.08m$, $y_{\min} = -0.24m$, $y_{\max} = 0.78m$ in the base frame.

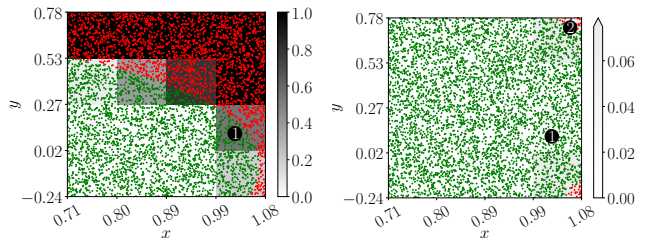
A. Incremental Acquisition of Demonstrations

To illustrate the application of Alg. 1 to incrementally acquire a sufficient set of demonstrations, we choose $\epsilon = 0.02$, $\delta = 0.05$, $\beta = 0.95$, and $K = 16$ for the experiments.

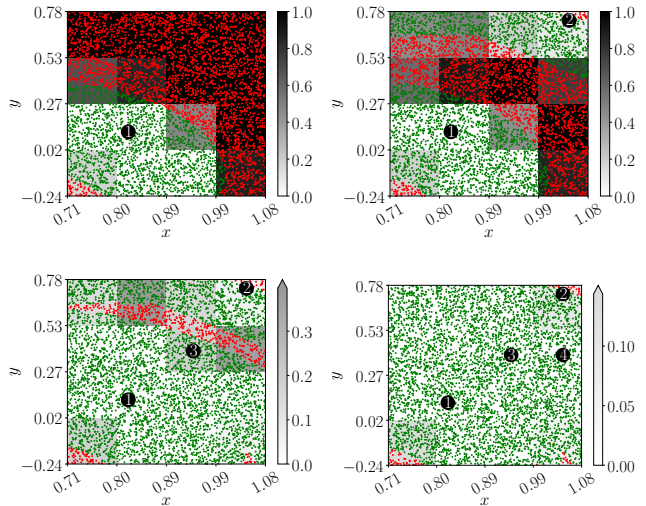
Fig. 4 shows the results of the experiment for **pouring** and **scooping**. In particular, Fig. 4(a) shows the two probability heat maps after incrementally acquiring 2 demonstrations for the **pouring** task. After acquiring the 1st demonstration (Fig. 4(a) left heat map), Alg. 1 picks the region with the highest failure probability (ties broken arbitrarily). In this case, the chosen region happens to be the one in the top right corner, from where we acquire the 2nd demonstration, and after collecting that, the failure probability heatmap evolves into the one shown to the right of Fig. 4(a). Similarly, in Fig. 4(b), we show the four failure-probability heat maps for the **scooping** task, after acquiring 4 demonstrations incrementally. The results indicate that *for pouring and scooping, respectively, 2 and 4 demonstrations are sufficient for the robot to have a belief that with probability 0.95 ($1 - \delta$), it can perform the task successfully for 95% (β) of the task instances in the given region \mathcal{X} .*

B. Effect of the Choice of K

The number of demonstrations obtained above may change with different executions and also depends on the choice of K . To get an idea of the distribution of the number of sufficient demonstrations, we performed 1000 tests using self-evaluation, each for a different value of the number



(a) Failure probability heat-map of the **pouring** task after incrementally adding kinesthetic demonstrations #1 and #2



(b) Failure probability heat-map of the **scooping** task after incrementally adding kinesthetic demonstrations #1, #2, #3, and #4

Fig. 4: Visualization of the robot’s change of belief about its ability to successfully perform tasks in the work area as it acquires demonstrations. The annotated black dots are the object locations during the demonstrations. The green and red dots are task instances for which plan generation succeeded and failed, respectively.

of disjoint regions K . The parameters ϵ , δ , and β were kept the same in all executions as before. Note that Alg. 1 is an interactive process in which after each iteration the robot asks for the next demonstration from a human until it achieves its desired confidence. For the purpose of this experiment and to bypass the human-robot interaction after each iteration, we pre-collected 32 demonstrations with at least 1 demonstration in any selected region. The result of the simulation is shown in Fig. 5. The distributions reveal that we need a maximum of 7 and 5 demonstrations for pouring and scooping, respectively. Furthermore, as K increases, the expected number of demonstrations increases marginally. Note that smaller values of K require a smaller number of samples (from the bandit formulation). However, with smaller values of K , although we may achieve the desired confidence in the entire work area, there may be regions with much lower local success probabilities. This phenomenon is explored in detail below.

The success rates in individual regions and the total number of demonstrations depend on the choice of the number of such regions, K . For smaller values of K , the lower number of demonstrations (see Fig. 5) is due to the fact that we had fewer task samples to evaluate and the

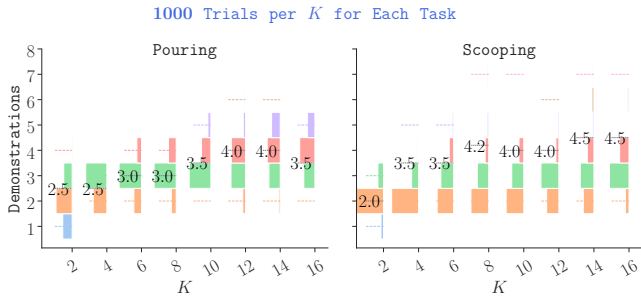


Fig. 5: Distribution (p.m.f) of demonstrations for different values of the number of regions K . For each K , the Self Evaluation plan generation in each region with a given probability that ultimately ensures overall success with high confidence.

success guarantee is also not fine-grained, in the sense that although the overall probability guarantee may be satisfied, there may be regions where the performance is poor. We have demonstrated this with an example in Fig. 6. With $K = 1$ (left), an overall success probability of 0.95 is achieved in the entire work area using only 2 demonstrations. However, resampling the work area with the same demonstrations but with a higher value of $K = 16$ (right) shows that there exists a failure-prone region in the bottom right corner with a low individual success probability of 0.6. The choice of K is application specific so that the requirement of being able to succeed (with high probability) in the overall work area alone can be met by choosing a smaller value of K . However, to identify the pockets of failure and to succeed in each individual region, one may need to choose a higher K , which in turn comes with the additional cost of a larger number of samples, as well as a few more demonstrations.

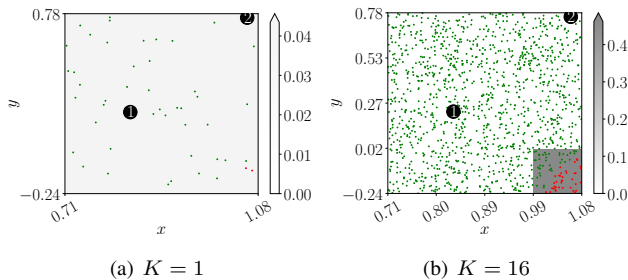


Fig. 6: Effect of choosing 2 different values of the number of disjoint regions K , but with the same demonstrations.

C. Experimental Validation of Manipulation Capability Over the Prescribed Work Area

In the results discussed thus far, sufficient sets of kinesthetic demonstrations were obtained using a robot, but plans for random task instances were evaluated via simulation. Next, we describe experiments to validate the simulation results by executing the generated plans on a robot.

For a given set of sufficient demonstrations, we generated random task instances over the workspace and a plan was generated for each task instance, demonstration pair. The first feasible plan (which did not violate the joint limits) was used to execute the task. We selected 32 random task instances (2 from each of the 16 subregions) for which plan generation was successful in simulation and executed the

generated plans. We did not observe execution failure in terms of joint limit violation in any of these executions.

VII. CONCLUSION AND FUTURE WORK

This paper presents a novel approach to systematically obtain a sufficient set of kinesthetic demonstrations for complex manipulation tasks, one example at a time, such that the robot can develop a probabilistic confidence bound in its ability to generate feasible manipulation plans. Inspired by multi-arm bandit strategies, we propose an algorithm to partition the work area into disjoint subregions, ensuring successful plan generation in each region with a given probability that ultimately ensures overall success with high confidence.

The number of regions of interest for demonstrations (and the task space) increases exponentially with the number of task-relevant objects. Consequently, for the algorithm `getBestArm` (Alg. 2) to scale well, we will need to use a combination of non-naive sampling methods such as adaptive sampling [35], and hierarchical methods to focus on smaller sets of promising candidates.

Finally, we are studying whether demonstrations given in one context can be reused in a new environment, i.e., a new work area or robot. In this setting, it is possible to collect additional demonstrations in the new environment using the performance of the reused demonstrations as prior knowledge. Techniques for effectively reusing demonstrations in different environments remain an area to be further explored.

REFERENCES

- [1] B. D. Argall, S. Chernova, M. Veloso, and B. Browning, "A survey of robot learning from demonstration," *Robotics and autonomous systems*, vol. 57, no. 5, pp. 469–483, 2009.
- [2] S. Chernova and A. L. Thomaz, *Robot learning from human teachers*. Morgan & Claypool Publishers, 2014.
- [3] S. Calinon, F. Guenter, and A. Billard, "On learning, representing, and generalizing a task in a humanoid robot," *Trans. on Systems, Man, and Cybernetics, Part B (Cybernetics)*, vol. 37, no. 2, pp. 286–298, 2007.
- [4] S. Calinon, F. D’halluin, E. L. Sauser, D. G. Caldwell, and A. G. Billard, "Learning and reproduction of gestures by imitation," *IEEE Robotics & Automation Magazine*, pp. 44–54, 2010.
- [5] S. Calinon, A. Pistillo, and D. G. Caldwell, "Encoding the time and space constraints of a task in explicit-duration hidden Markov model," in *Intelligent Robots and Systems*. IEEE, 2011, pp. 3413–3418.
- [6] K. Fischer, F. Kirstein, L. C. Jensen, N. Krüger, K. Kukliński, M. V. aus der Wieschen, and T. R. Savarimuthu, "A comparison of types of robot control for programming by demonstration," *HRI*, pp. 213–220, 2016.
- [7] C. Pérez-D’Arpino and J. A. Shah, "C-learn: Learning geometric constraints for multi-step manipulation in shared autonomy," in *ICRA*, 2017, pp. 4058–4065.
- [8] E. G. Herrero, J. Ho, and O. Khatib, "Understanding and segmenting human demonstrations into reusable compliant primitives," in *IROS*, 2021.
- [9] S. Bahl, A. Gupta, and D. Pathak, "Hierarchical neural dynamic policies," in *Robotics: Science and Systems*, 2021.
- [10] T. Yu and Q. Chang, "User-guided motion planning with reinforcement learning for human-robot collaboration in smart manufacturing," *Expert Systems with Applications*, p. 118291, 2022.
- [11] Z. Fu, T. Z. Zhao, and C. Finn, "Mobile ALOHA: Learning bimanual mobile manipulation with low-cost whole-body teleoperation," in *CoRL*, 2024.
- [12] J. Wang, C.-C. Chang, J. Duan, D. Fox, and R. Krishna, "EVE: Enabling anyone to train robots using augmented reality," in *UIST*, 2024, pp. 1–13.
- [13] B. Zitkovich *et al.*, "RT-2: Vision-language-action models transfer web knowledge to robotic control," in *CoRL*, 2023, pp. 2165–2183.

- [14] R. Laha, A. Rao, L. F. Figueredo, Q. Chang, S. Haddadin, and N. Chakraborty, "Point-to-point path planning based on user guidance and screw linear interpolation," in *Intl Design Engg. Tech, Conf. and Comp. and Info. in Engg. Conf.*, vol. 85451. ASME, 2021.
- [15] D. Mahalingam and N. Chakraborty, "Human-guided planning for complex manipulation tasks using the screw geometry of motion," in *ICRA*, 2023, pp. 7851–7857.
- [16] A. Sarker, A. Sinha, and N. Chakraborty, "On screw linear interpolation for point-to-point path planning," in *IROS*, 2020, pp. 9480–9487.
- [17] E. Even-Dar, S. Mannor, and Y. Mansour, "PAC bounds for multi-armed bandit and markov decision processes," in *CoLT*. Springer, 2002, pp. 255–270.
- [18] A. G. Billard, S. Calinon, and R. Dillmann, "Learning from humans," *Springer handbook of robotics*, pp. 1995–2014, 2016.
- [19] D. Kulić, C. Ott, D. Lee, J. Ishikawa, and Y. Nakamura, "Incremental learning of full body motion primitives and their sequencing through human motion observation," *The International Journal of Robotics Research*, pp. 330–345, 2012.
- [20] S. Calinon and A. Billard, "Statistical learning by imitation of competing constraints in joint space and task space," *Advanced Robotics*, vol. 23, no. 15, pp. 2059–2076, 2009.
- [21] M. Hersch, F. Guenter, S. Calinon, and A. Billard, "Dynamical system modulation for robot learning via kinesthetic demonstrations," *IEEE Transactions on Robotics*, vol. 24, no. 6, pp. 1463–1467, 2008.
- [22] P. Pastor, H. Hoffmann, T. Asfour, and S. Schaal, "Learning and generalization of motor skills by learning from demonstration," in *ICRA*, 2009, pp. 763–768.
- [23] M. Saveriano, F. Franzel, and D. Lee, "Merging position and orientation motion primitives," in *ICRA*, 2019, pp. 7041–7047.
- [24] A. J. Ijspeert, J. Nakanishi, H. Hoffmann, P. Pastor, and S. Schaal, "Dynamical movement primitives: learning attractor models for motor behaviors," *Neural computation*, vol. 25, no. 2, pp. 328–373, 2013.
- [25] R. Chatila, E. Renaudo *et al.*, "Toward self-aware robots," *Frontiers in Robotics and AI*, vol. 5, p. 88, 2018.
- [26] A. Gautam, T. Whiting, X. Cao, M. A. Goodrich, and J. W. Crandall, "A method for designing autonomous robots that know their limits," in *ICRA*, 2022, pp. 121–127.
- [27] M. Zillich, J. Prankl, T. Mörwald, and M. Vincze, "Knowing your limits-self-evaluation and prediction in object recognition," in *IROS*, 2011, pp. 813–820.
- [28] K. N. Kaipa, A. S. Kankanalli-Nagendra, and S. K. Gupta, "Toward estimating task execution confidence for robotic bin-picking applications," in *AAAI*, 2015.
- [29] T. Frasca and M. Scheutz, "A framework for robot self-assessment of expected task performance," *IEEE Robotics and Automation Letters*, vol. 7, no. 4, pp. 12523–12530, 2022.
- [30] T. Trinh, H. Chen, and D. S. Brown, "Autonomous assessment of demonstration sufficiency via Bayesian inverse reinforcement learning," in *HRI*, 2024, pp. 725–733.
- [31] G. S. Chirikjian and A. B. Kyatkin, *Harmonic analysis for engineers and applied scientists: updated and expanded edition*. Courier Dover Publications, 2016.
- [32] A. Garivier and E. Kaufmann, "Optimal best arm identification with fixed confidence," in *CoLT*, 2016, pp. 998–1027.
- [33] J. J. Kuffner, "Effective sampling and distance metrics for 3D rigid body path planning," in *IEEE ICRA*, vol. 4, 2004, pp. 3993–3998.
- [34] S. Mannor and J. N. Tsitsiklis, "The sample complexity of exploration in the multi-armed bandit problem," *Journal of Machine Learning Research*, vol. 5, no. Jun, pp. 623–648, 2004.
- [35] P. Auer, N. Cesa-Bianchi, and P. Fischer, "Finite-time analysis of the multiarmed bandit problem," *Machine Learning*, vol. 47, no. 2, pp. 235–256, 2002.

APPENDIX

A. Identification of an ϵ -Optimal Arm in K -Arm Bandit

Given K arms with unknown binary reward distributions R_j , $j \in [1, K]$, where $\mu_j = \mathbb{E}[R_j]$, the objective is to identify an arm 'a' which is ϵ -close to the optimal arm i.e. $\max_j \{\mu_j\} - \mu_a \leq \epsilon$.

Alg. 3 gives a natural way to detect the arm with the highest expected reward by sampling each arm an equal

number of times, say $\frac{T}{K}$, for a given number of samples T , and output the arm with the best empirical mean.

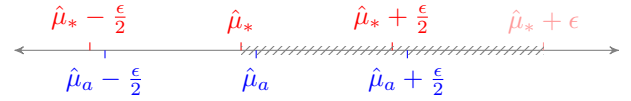
Algorithm 3 ϵ -optimal arm identification in K -arm bandit

- Step 1: Collect $\lfloor \frac{T}{K} \rfloor$ samples from each of the K arms
 Step 2: Calculate empirical means $\hat{\mu}_1, \hat{\mu}_2, \dots, \hat{\mu}_K$ and output $\arg \max_j \{\hat{\mu}_j\}$
-

Theorem 1.1: Algorithm 3 is correct if $|\mu_j - \hat{\mu}_j| \leq \epsilon/2 \quad \forall j \in [1, K]$.

Proof: We assume '*' is the unidentified optimal arm, that is, $\forall j, \mu_* \geq \mu_j$ and 'a' is the arm found by Algorithm 3, that is $\forall j, \hat{\mu}_a \geq \hat{\mu}_j$. We need to show that $\mu_* - \mu_a \leq \epsilon$.

Only $\hat{\mu}_a \in [\hat{\mu}_*, \hat{\mu}_* + \epsilon]$ (the hatched interval below) is consistent with our previous assumption as observed below.



Thus, from the above diagram it is obvious that, $\hat{\mu}_a - \frac{\epsilon}{2} \leq \mu_a \leq \mu_* \leq \hat{\mu}_* + \frac{\epsilon}{2}$. Therefore, the difference between μ_* and μ_a is the maximum when $\mu_a = \hat{\mu}_a - \frac{\epsilon}{2}$ and $\mu_* = \hat{\mu}_* + \frac{\epsilon}{2}$ and the maximum difference is ϵ .

Hence, $\mu_* - \mu_a \leq \epsilon$ that is, if $|\mu_j - \hat{\mu}_j| \leq \epsilon/2 \quad \forall j \in [1, K]$, Algorithm 3 always returns an ϵ -optimal arm. ■

Theorem 1.2: Algorithm 3 returns an ϵ -optimal arm with a probability of at least $1 - 2Ke^{-\frac{T\epsilon^2}{2K}}$

Proof: Let E_j be the event $|\mu_j - \hat{\mu}_j| \leq \epsilon/2$. Thus, Alg. 3 outputs the correct arm, i.e. an ϵ -optimal arm 'a' with probability

$$\begin{aligned} \mathbb{P}\left(\bigcap_{i=1}^K E_j\right) &= 1 - \mathbb{P}\left(\bigcup_{i=1}^K E_j^c\right) \quad [E_j^c \text{ is complement of } E_j] \\ &\geq 1 - \sum_{i=1}^K \mathbb{P}(E_j^c) \left[\cdot: \mathbb{P}\left(\bigcup_{i=1}^K A_i\right) \leq \sum_{i=1}^K \mathbb{P}(A_i) \right] \quad (4) \end{aligned}$$

Using the Hoeffding-Chernoff inequality for Bernoulli random variable R_j with true-mean μ_j and estimated-mean $\hat{\mu}_j$ determined using $\frac{T}{K}$ samples, we get

$$\mathbb{P}\left(|\mu_j - \hat{\mu}_j| \leq \frac{\epsilon}{2}\right) \geq 1 - 2e^{-\frac{2T\epsilon^2}{4K}} \quad \forall j \in [1, K]$$

$$\mathbb{P}(E_j) \geq 1 - 2e^{-\frac{T\epsilon^2}{2K}}$$

$$\mathbb{P}(E_j^c) \leq 2e^{-\frac{T\epsilon^2}{2K}} \quad (5)$$

Substituting (5) in (4), we get $\mathbb{P}\left(\bigcap_{i=1}^K E_j\right) \geq 1 - 2Ke^{-\frac{T\epsilon^2}{2K}}$
 Hence, Algorithm 3 outputs an ϵ -optimal arm with a probability of at least $1 - 2Ke^{-\frac{T\epsilon^2}{2K}}$. ■

Corollary 2.1: For Alg. 3 to succeed with a probability of at least $1 - \delta$, the number of samples T should be at least $\frac{2K}{\epsilon^2} \ln\left(\frac{2K}{\delta}\right)$.

Substituting $2Ke^{-\frac{T\epsilon^2}{2K}}$ by δ in Theorem 1.2 gives us an (ϵ, δ) -PAC bound, in which using at least $\frac{2K}{\epsilon^2} \ln\left(\frac{2K}{\delta}\right)$ samples we can identify an ϵ -optimal arm with a confidence of at least $1 - \delta$.